

# Faraday Discussions

Accepted Manuscript



This is an Accepted Manuscript, which has been through the Royal Society of Chemistry peer review process and has been accepted for publication.

Accepted Manuscripts are published online shortly after acceptance, before technical editing, formatting and proof reading. Using this free service, authors can make their results available to the community, in citable form, before we publish the edited article. We will replace this Accepted Manuscript with the edited and formatted Advance Article as soon as it is available.

You can find more information about Accepted Manuscripts in the [Information for Authors](#).

Please note that technical editing may introduce minor changes to the text and/or graphics, which may alter content. The journal's standard [Terms & Conditions](#) and the [Ethical guidelines](#) still apply. In no event shall the Royal Society of Chemistry be held responsible for any errors or omissions in this Accepted Manuscript or any consequences arising from the use of any information it contains.

This article can be cited before page numbers have been issued, to do this please use: A. McCullagh and D. Lennon, *Faraday Discuss.*, 2026, DOI: 10.1039/D5FD00169B.

Paper for submission to:

RSC Faraday Discussion, Vibrations at Interfaces

Draft:

16<sup>th</sup> January 2025 View Article Online  
DOI: 10.1039/D5FD00169B

# Co-adsorption of aniline and H<sub>2</sub> over Pd/Al<sub>2</sub>O<sub>3</sub>: An infrared spectroscopic study

Annelouise M. McCullagh and David Lennon \*

School of Chemistry, Joseph Black Building, University of Glasgow, Glasgow, G12 8QQ, UK.

\* Proofs to:–

Professor David Lennon CChem, FRSC  
School of Chemistry  
Joseph Black Building  
The University of Glasgow  
Glasgow, G12 8QQ, U.K.

Email: David.Lennon@glasgow.ac.uk

Telephone: +44-141-330-4372



## Abstract

View Article Online  
DOI: 10.1039/D5FD00169B

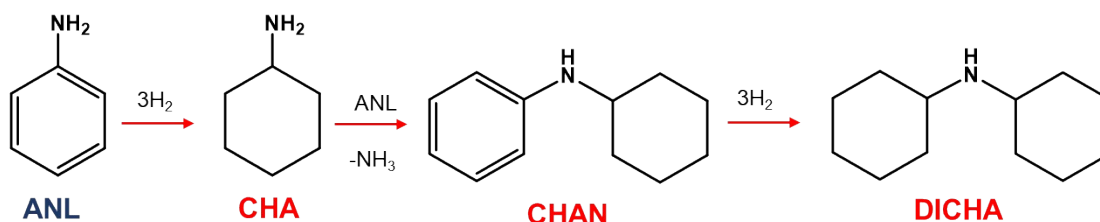
In order to rationalise high aniline selectivity in nitrobenzene hydrogenation over alumina-supported Pd catalysts, the adsorption complex geometry of aniline during co-adsorption of H<sub>2</sub> and aniline on a 5 wt % Pd/Al<sub>2</sub>O<sub>3</sub> catalyst is investigated via infrared spectroscopy. With respect to molecular symmetry and the metal surface selection rule, observation of solely out-of-plane aniline modes at low aniline exposures at 30 °C indicate a parallel orientation of aniline with respect to the Pd surface. The simultaneous emergence of negative hydroxyl features indicate adsorption occurs at the metal/support interface. Increasing exposure reveals additional adsorption of aniline to a range of hydroxyls of the alumina support. The full range of adsorption spectra reveal that the presence of H<sub>2</sub> in the co-feed accelerates aniline adsorption to the catalyst and permits reagent hydrogenation to cyclohexylamine. Temperature-programmed infrared measurements show no change in the adsorption complex geometry as a function of surface coverage. A previous reaction scheme is modified in which nitrobenzene and aniline adsorption geometry are intrinsically related to the high aniline selectivity reported for Pd/Al<sub>2</sub>O<sub>3</sub> catalysts.



# 1. Introduction

View Article Online  
DOI: 10.1039/D5FD00169B

Aniline synthesis catalysis via nitrobenzene hydrogenation is an established reaction of some significance<sup>1–6</sup>. Not least, as part of the production chain for the manufacture of methylene diphenyl diisocyanate, a key component in polyurethane production<sup>7</sup>. Recent work by the authors has examined the case for the application of Pd/Al<sub>2</sub>O<sub>3</sub> as an aniline synthesis catalyst, that is able to facilitate highly selective aniline synthesis in nitrobenzene hydrogenation, with over-hydrogenation of aniline identified as the principal route to by-product formation<sup>2,6,8,9</sup>. This over-hydrogenation is a three-step process producing cyclohexylamine (CHA), from hydrogenation of the aniline aromatic ring, N-cyclohexylaniline (CHAN), from coupling of aniline and CHA, and finally dicyclohexylamine (DICHA) from hydrogenation of the aromatic moiety of CHAN (Scheme 1).



**Scheme 1.** Aniline hydrogenation to cyclohexylamine (CHA), N-cyclohexylaniline (CHAN) and dicyclohexylamine (DICHA). Adapted from reference<sup>6</sup> Copyright – CC BY 4.0.

Aniline comprises an aromatic ring and an amine group, both inherently capable of interacting with metal surfaces, potentially influencing adsorption geometry and catalytic performance. Surface science has proved influential in understanding adsorbate/substrate bonding configurations. For example, Rockey *et al.* examined aniline adsorption on Ag(111) using high-resolution electron energy loss spectroscopy<sup>10</sup>. Two distinct peaks were observed: an out-of-plane ring deformation at 486 cm<sup>-1</sup> and an out-of-plane C–H bend at 737 cm<sup>-1</sup>. The absence of in-plane modes indicated parallel adsorption, with spectral deconvolution estimating a tilt angle of 13 ± 8°, and adsorption proposed to occur via the amino group.

Huang *et al.* explored aniline orientation and hydrogenolysis species on Pt(111) using temperature-programmed reaction and NEXAFS<sup>11</sup>. Analysis of π\* and σ\* resonance intensities relative to incidence angle revealed that, in the absence of hydrogen, the aromatic ring was tilted with respect to Pt(111), with a maximum tilt of ~31°; π-Bonding between the ring and Pt dominated under these conditions.



In contrast, hydrogen co-adsorption induced a predominantly parallel orientation, suggesting stronger interaction involving both  $\pi$ -electrons and the nitrogen lone pair. Thus, hydrogen significantly influences both orientation and binding strength.

View Article Online

DOI: 10.1039/D3FD00169B

Computational studies corroborate these findings. Alsunaidi *et al.* reported parallel adsorption of aniline on Ni(111) during benzene amination, with C–H bonds buckled away from the surface<sup>12</sup>. Binding involved  $\pi$ -interactions at bridging sites and  $\sigma$ -interactions at on-top sites via NH<sub>2</sub>. Similar configurations were predicted by Tezsevin *et al.* for Ru(0001) and Co(0001)<sup>13</sup>, and by Henríquez-Román *et al.* for Cu defect sites, including steps, kinks, and corners<sup>14</sup>.

Regarding aniline adsorption on supported metal catalysts, previous work by the authors used infrared spectroscopy to examine nitrobenzene adsorption on a 5 wt% Pd/Al<sub>2</sub>O<sub>3</sub> catalyst and established nitrobenzene to adopt a vertical monodentate adsorption geometry on the Pd crystallites, alongside aniline re-adsorption onto the inactive alumina support through hydrogen bonding with surface hydroxyls<sup>15</sup>. An investigation into structure-activity relationships for Pd/Al<sub>2</sub>O<sub>3</sub> catalysts during nitrobenzene hydrogenation identified the concomitant shut down of aniline over-hydrogenation chemistry with poisoning of the Pd(100) site<sup>8</sup>. Thus, it was postulated that nitrobenzene hydrogenation activity occurs on the dominant Pd(111) facets, whilst aniline hydrogenation is facilitated by the minimised Pd(100) facets. Furthering this, a combined spectroscopic and computational investigation on sole aniline adsorption on Pd/Al<sub>2</sub>O<sub>3</sub> confirmed aniline adsorption on the inactive alumina support alongside parallel aniline adsorption at the Pd(100)/support interfacial sites<sup>16</sup>.

Recent reaction testing of aniline hydrogenation over the same Pd/Al<sub>2</sub>O<sub>3</sub> catalyst demonstrated low activity in strongly reducing conditions at elevated temperature<sup>17</sup>. Whereas qualitatively, this outcome verifies low aniline-derived by-products in nitrobenzene hydrogenation over supported Pd catalysts, nevertheless there is a driver to rationalise such favourable outcomes in terms of adsorbate geometry under actual reaction conditions. Against this background, the present study investigates aniline adsorption geometry over the aforementioned 5 wt% Pd/Al<sub>2</sub>O<sub>3</sub> catalyst with a hydrogen co-feed, *i.e.* during catalytic turnover, to advance understanding of the origins of high aniline selectivity over Pd catalysts under hydrogenation conditions.



## 2. Experimental

View Article Online  
DOI: 10.1039/D5FD00169B

*In situ* diffuse-reflectance infrared Fourier transform spectroscopy (DRIFTS) measurements were conducted using a Bruker Vertex 70 FT-IR spectrometer equipped with an MCT detector. The catalyst (5 wt% Pd/Al<sub>2</sub>O<sub>3</sub>; Alfa Aesar: 11713) was used as-received in powder form, with approximately 50 mg placed in a Harrick Praying Mantis reaction chamber fitted with an ATC heater for temperature control.

Catalyst activation was performed *in situ* under a flow of helium (35 mL min<sup>-1</sup>, BOC, 99.9%) and hydrogen (15 mL min<sup>-1</sup>, BOC, 99.8%) while heating to 110 °C, held for 30 min. The temperature was then increased to 200 °C for 1 h, with hydrogen flow stopped after 30 min. The sample was cooled to ambient temperature under helium and purged for 18 h to minimize residual hydrogen, which could otherwise promote uncontrolled aniline hydrogenation. A background spectrum was recorded at 28 °C.

Aniline was introduced via a bubbler system delivering 54.0 μmol(ANL) min<sup>-1</sup> g(cat)<sup>-1</sup> in the vapor phase using helium as the carrier gas. Hydrogen was introduced to the cell via a mass flow controller (Brooks) delivering 1.37 mmol(H<sub>2</sub>) min<sup>-1</sup> g(cat)<sup>-1</sup>. Spectra (aniline:H<sub>2</sub> = 1:25 v/v) were collected at defined intervals during adsorption to quantify aniline uptake. For desorption studies, the catalyst was heated under helium to the target temperature, held for 30 min, then cooled to 28 °C for spectral acquisition. This procedure was repeated for 60, 100, 120, 160, and 200 °C. All spectra were recorded at 30 °C using 520 scans at 4 cm<sup>-1</sup> resolution and presented as difference spectra (activated catalyst spectrum subtracted from aniline-dosed spectrum) without additional processing.

## 3. Results

Key aniline modes for orientational diagnostics were assigned by the authors previously<sup>16</sup>. These are the ν(Ph-NH<sub>2</sub>), ν(CC) [24], ν(CC) [4], and δ<sub>oop</sub>(NH<sub>2</sub>) modes observed at *ca.* 1280, 1500, 1600 and 1620 cm<sup>-1</sup>, respectively. Table S1 in the Supporting Information presents wavenumber assignments.

### 3.1 Adsorption Geometry: Function of Aniline & H<sub>2</sub> Surface Coverage

Incremental co-adsorption of aniline (exposures 0.11–4.86 mmol g(cat)<sup>-1</sup>) and hydrogen (exposures 2.75–122 mmol g(cat)<sup>-1</sup>) on 5 wt% Pd/Al<sub>2</sub>O<sub>3</sub> produced spectra (Figure 1) that reveal both adsorbed aniline and hydrogenation products.



At low reagent exposures ( $\leq 0.54 \text{ mmol}_{(\text{ANL})}$  and  $13.5 \text{ mmol}_{(\text{H}_2)}$ ) the following features are noted: (i) a broad peak at *ca.*  $1640 \text{ cm}^{-1}$  assigned to  $\delta_{\text{oop}}(\text{NH}_2)$ , (ii) a broad feature from  $3500 - 3000 \text{ cm}^{-1}$  associated with aniline  $\text{NH}_2$  hydrogen bonding to the catalyst and (iii) negative hydroxyl features at *ca.*  $3750 - 3650 \text{ cm}^{-1}$ . The absence of in-plane aniline modes is indicative of a parallel adsorption of aniline at the metal surface. Due to the background subtraction procedure deployed (Section 2), the negative hydroxyl features represent perturbation of alumina surface hydroxyls after aniline adsorption and identifies these hydroxyls as an adsorption site <sup>16</sup>. The coincidence of aniline adsorption parallel to the Pd surface and aniline adsorption at support hydroxyls indicates adsorption at the metal/support interface under this coverage regime.

At maximum exposure, all key aniline modes are evident: in-plane  $A'$   $\nu(\text{CC})$  and  $\nu(\text{Ph-NH}_2)$  at  $1601$  and  $1278 \text{ cm}^{-1}$ , in-plane  $A''$   $\nu(\text{CC})$  at  $1500 \text{ cm}^{-1}$ , and out-of-plane  $A'$   $\delta_{\text{oop}}(\text{NH}_2)$  at  $1628 \text{ cm}^{-1}$ . Collectively, these modes match the spectrum for sole aniline adsorption to the alumina support, as reported previously <sup>16</sup>. However, two additional sharp bands at  $2934$  and  $2852 \text{ cm}^{-1}$  are noted, and are assigned to the  $\nu_{\text{AS}}(\text{CH}_2)$  and  $\nu_{\text{S}}(\text{CH}_2)$  of cyclohexylamine (CHA), confirming partial hydrogenation of aniline in the presence of hydrogen <sup>18,19</sup>.

Peak area analysis (Figure S1, Supporting Information) shows aniline approaching saturation, while CHA bands increase continuously with coverage. This divergence of profiles is indicative of adsorption occurring on distinct sites: (i) aniline adsorption involves hydroxyl groups and  $\text{Pd}(100)^8/\text{support}$  interface, and (ii) CHA on additional sites. The attribution that the aniline metal adsorption site is  $\text{Pd}(100)$  facets originates from McCullagh and co-workers' study of solely aniline adsorption on  $\text{Pd}/\text{Al}_2\text{O}_3$ .<sup>16</sup> On the basis of relative peak intensities, CHA formation remains minor compared to aniline adsorption; this is consistent with reaction testing outcomes <sup>17</sup>. This mechanistic insight underscores the role of hydrogen in modifying adsorption geometry and promoting transformation pathways on  $\text{Pd}/\gamma\text{-Al}_2\text{O}_3$ . Literature comparison indicates CHA adopts the equatorial conformer under these conditions, supported by  $\nu_{\text{AS}}(\text{CH}_2)$  at  $2934 \text{ cm}^{-1}$  <sup>13</sup>.



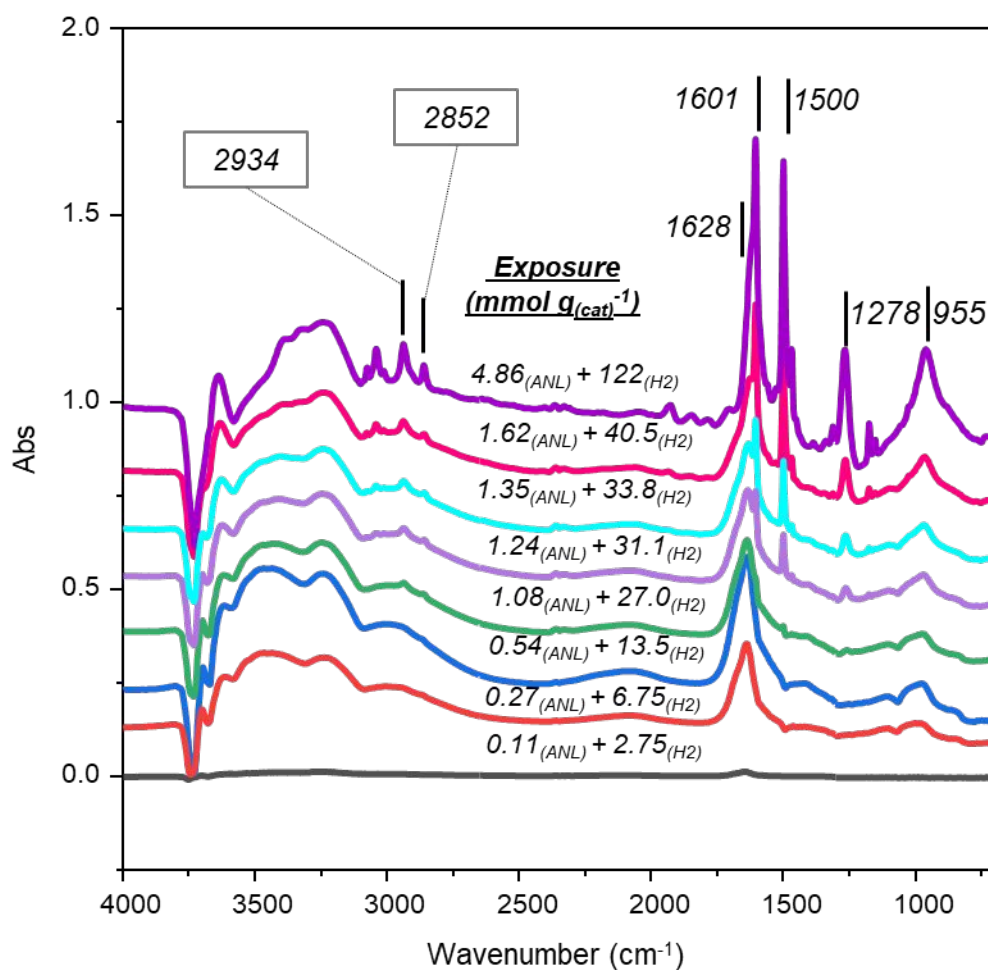
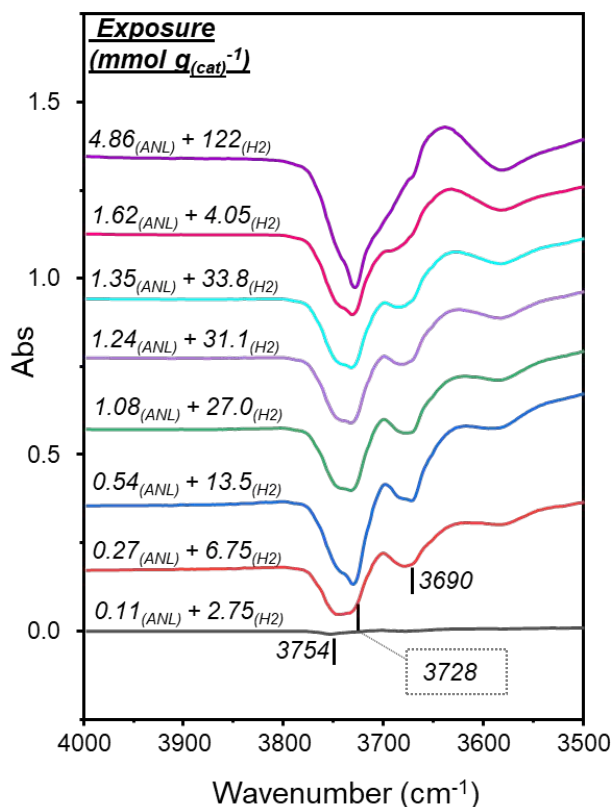


**Figure 1.** DRIFTS spectra ( $4000 - 700 \text{ cm}^{-1}$ ) depicting increasing aniline and hydrogen ( $0.11 - 4.86 \text{ mmol}_{(ANL)} \text{ g}_{(cat)}^{-1}$  and  $2.75 - 122 \text{ mmol}_{(H_2)} \text{ g}_{(cat)}^{-1}$ ) exposure to  $\text{Pd}/\text{Al}_2\text{O}_3$  at  $30^\circ\text{C}$ . The spectra have been offset to facilitate viewing.





View Article Online  
DOI: 10.1039/D5FD00169B

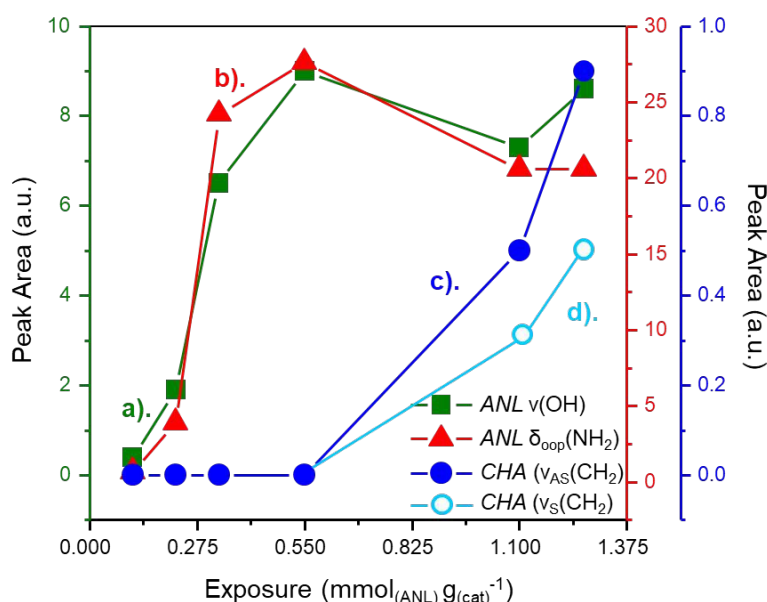
**Figure 2.** DRIFTS spectra ( $4000 - 3500 \text{ cm}^{-1}$ ) depicting the hydroxyl group stretching region during increasing aniline and hydrogen ( $0.11 - 4.86 \text{ mmol}_{(ANL)} \text{ g}_{(cat)}^{-1}$  and  $2.75 - 122 \text{ mmol}_{(H2)} \text{ g}_{(cat)}^{-1}$ ) exposure to  $\text{Pd}/\text{Al}_2\text{O}_3$  at  $30 \text{ }^\circ\text{C}$ . The spectra have been offset to facilitate viewing.

Figure 2 presents the hydroxyl stretch region during co-adsorption of aniline and hydrogen to the catalyst and reproduces trends comparable to those reported for sole aniline adsorption over  $\text{Pd}/\text{Al}_2\text{O}_3$ <sup>16</sup>. Specifically, negative features depicted at  $3754$ ,  $3728$  and  $3690 \text{ cm}^{-1}$  are associated with H-bonded type IIa, type IIb and type III hydroxyl groups, respectively<sup>20</sup>. Thus, during co-adsorption with hydrogen, aniline is partitioned over the same three hydroxyl groups present on the inactive  $\gamma\text{-Al}_2\text{O}_3$  support via H-bonding.

Some differences in the  $\nu(\text{O-H})$  band profiles for sole aniline adsorption<sup>16</sup> and aniline/hydrogen co-adsorption are noted. Specifically, the negative feature at *ca.*  $3728 \text{ cm}^{-1}$ , attributable to type IIb hydroxyl groups<sup>20</sup>, is observable at lower exposures in the co-adsorption measurements and remains prominent at higher exposures. It is therefore assumed that the presence of hydrogen in the co-feed is facilitating H-bonding to the hydroxyl groups of the alumina support.



Figure 3 presents IR peak areas of diagnostic aniline and CHA bands in the lower exposure range (0.11(ANL) + 2.75(H<sub>2</sub>) to 1.24(ANL) + 31.1(H<sub>2</sub>) mmol g(cat)<sup>-1</sup>). For clarity, the negative  $\nu(\text{OH})$  feature—indicative of H-bonding between Pd/Al<sub>2</sub>O<sub>3</sub> hydroxyls and aniline—is plotted as a positive value, so an increase reflects stronger H-bonding. Peak areas for  $\nu(\text{OH})$  (Figure 3a) and the aniline  $\delta_{\text{oop}}(\text{NH}_2)$  mode (Figure 3b) follow the same trend, seeming to plateau at an aniline exposure of about 0.40 mmol g(cat)<sup>-1</sup>; the bonding here is attributed to adsorption at Pd/support interfacial sites. The ‘knee’ in the profile of the  $\nu(\text{OH})$  and  $\delta_{\text{oop}}(\text{NH}_2)$  modes roughly coincides with the emergence of CHA  $\nu_{\text{AS}}(\text{CH}_2)$  (Figure 3c) and  $\nu_{\text{S}}(\text{CH}_2)$  (Figure 3d) bands. This inverse relationship is indicative of aniline adsorbed in a parallel orientation at Pd(100)/support interface undergoing hydrogenation to CHA on saturation. Thus, hydrogenation occurs upon saturation of the interfacial species.



**Figure 3.** Plot of peak area for bands corresponding to the a) H-bonded  $\nu(\text{OH})$  of Pd/Al<sub>2</sub>O<sub>3</sub>, b) the aniline  $\delta_{\text{oop}}(\text{NH}_2)$  mode, and the cyclohexylamine c)  $\nu_{\text{AS}}(\text{CH}_2)$  and d)  $\nu_{\text{S}}(\text{CH}_2)$  modes as a function of increasing aniline and H<sub>2</sub> exposure to 5 wt% Pd/Al<sub>2</sub>O<sub>3</sub>. Note: x-axis displays aniline exposure only.

For exposures > 1.13(ANL) + 28.4(H<sub>2</sub>) mmol g(cat)<sup>-1</sup>, the  $\nu(\text{OH})$  (Figure 3a) and the aniline  $\delta_{\text{oop}}(\text{NH}_2)$  (Figure 3b) modes diverge, with the  $\nu(\text{OH})$  mode showing continued augmentation, whilst the peak area for the aniline  $\delta_{\text{oop}}(\text{NH}_2)$  mode is unchanged. As per Figure 1, bands corresponding to in-plane modes of aniline, an indication of aniline adsorption to hydroxyl groups in isolation from the Pd crystallites, were first observable post-exposure of 1.13(ANL) + 28.4(H<sub>2</sub>) mmol g(cat)<sup>-1</sup>. Therefore, the observed variance of trends associated with peak area of the  $\nu(\text{OH})$  and aniline  $\delta_{\text{oop}}(\text{NH}_2)$  modes reflects continued adsorption of aniline to the hydroxyl groups of the alumina support, whilst adsorption of aniline at the Pd(100)/support interfacial sites saturates, reaching a steady state between aniline adsorption and hydrogenation to CHA.



### 3.2 Comparison of Aniline Adsorption to Pd/Al<sub>2</sub>O<sub>3</sub> With and Without Hydrogen

Figure 4 compares spectra collected after exposures of 0.54 and 1.62 mmol<sub>(ANL)</sub> g<sub>(cat)</sub><sup>-1</sup> with and without hydrogen and reveals notable differences at low coverage. At the low exposure (0.54 mmol<sub>(ANL)</sub> g<sub>(cat)</sub><sup>-1</sup>), the presence of hydrogen produces stronger negative hydroxyl features, a broad region between 3650–3000 cm<sup>-1</sup> encompassing  $\nu_{AS}(\text{NH}_2)$  and  $\nu_S(\text{NH}_2)$  modes, and a pronounced band at 1647 cm<sup>-1</sup>, compared to adsorption without hydrogen. In contrast, the higher exposure spectra (1.62 mmol<sub>(ANL)</sub> g<sub>(cat)</sub><sup>-1</sup>) -where adsorption continues to increase—show broadly similar profiles, with the hydrogen-free spectrum (Figure 4b) exhibiting a higher intensity aniline band. These trends are thought to indicate that the differences in spectral profiles noted at the lower exposure arise from ANL hydrogenation to CHA.

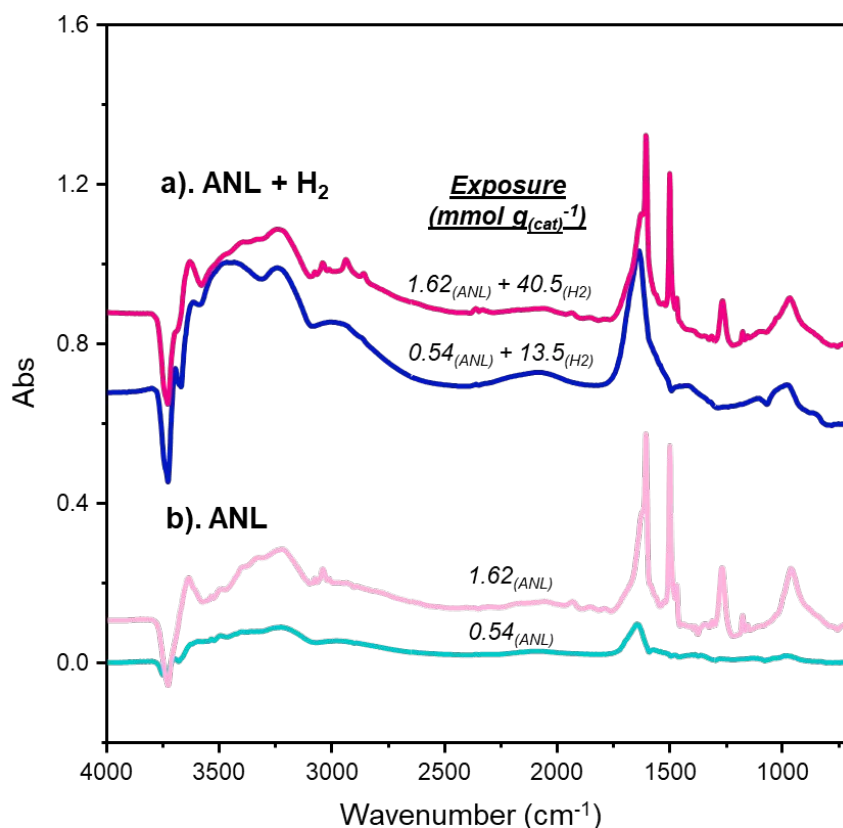


**Figure 4.** DRIFTS spectra corresponding to 0.54 and 1.62 mmol<sub>(ANL)</sub> g<sub>(cat)</sub><sup>-1</sup> exposures to Pd/Al<sub>2</sub>O<sub>3</sub> at 30 °C: a). with a H<sub>2</sub> co-feed and b). in the absence of a H<sub>2</sub> co-feed. The spectra have been offset to facilitate viewing. No additional manipulations were performed.

The primary difference associated with adsorption with and without hydrogen is the formation of CHA. CHA, like aniline, contains NH<sub>2</sub> functionality, with  $\nu_{AS}(\text{NH}_2)$  and  $\nu_S(\text{NH}_2)$  at 3352 and 3274 cm<sup>-1</sup>, respectively. In addition, CHA presents two in-plane NH<sub>2</sub> deformation modes ( $\delta_{ip}(\text{NH}_2)$ ) associated



with a shoulder feature at  $3170\text{ cm}^{-1}$  and a medium intensity feature at  $1617\text{ cm}^{-1}$ . Thus, the augmented broad feature at  $1647\text{ cm}^{-1}$  and enhanced  $\text{NH}_2$  stretching region seen in Figure 4 are likely to reflect CHA adsorption alongside aniline.

View Article Online  
DOI: 10.1039/D5FD00169B

Given prior evidence that CHA and aniline occupy different sites, it is intriguing to speculate on the bonding geometry of bound CHA. With reference to the metal surface selection rule (MSSR)<sup>21</sup>, the adsorption geometry of CHA on Pd(100) facets may also be hypothesized. Figures 1 and 4 present a significant contribution from the  $\delta_{\text{ip}}(\text{NH}_2)$  CHA modes compared to the usually high intensity  $\nu_{\text{AS}}(\text{CH}_2)$  and  $\nu_{\text{S}}(\text{CH}_2)$  modes. In relation to dipole orientation, the  $\nu_{\text{AS}}(\text{CH}_2)$  and  $\nu_{\text{S}}(\text{CH}_2)$  modes possess dipoles which are out-of-plane with respect to the molecular axis at an angle  $< 90^\circ$ . Contrarily, the  $\delta_{\text{ip}}(\text{NH}_2)$  modes possess dipoles aligned directly with the molecular axis. Thus, during a vertical adsorption of CHA over a metal surface, the  $\delta_{\text{ip}}(\text{NH}_2)$  modes would experience significant augmentation from the perpendicular alignment of associated dipoles with the metal surface; whilst the out-of-plane  $\nu_{\text{AS}}(\text{CH}_2)$  and  $\nu_{\text{S}}(\text{CH}_2)$  modes would undergo slight, but not complete, shielding due to the out-of-plane elements of their associated dipole moments. Therefore, a suggested assignment of CHA adsorption geometry on Pd/ $\text{Al}_2\text{O}_3$  is via vertical adsorption to the Pd(100) facets.

Moreover, both the in-plane  $\delta_{\text{ip}}(\text{NH}_2)$  of CHA<sup>18</sup> and the out-of-plane  $\delta_{\text{oop}}(\text{NH}_2)$  of aniline<sup>16</sup> are reported to occur at *ca.*  $1620\text{ cm}^{-1}$ . Thus, emergence of the combination of these modes at  $1647\text{ cm}^{-1}$  represents a noticeable shift ( $27\text{ cm}^{-1}$ ). Therefore, binding is proposed to arise via the  $\text{NH}_2$  functionality of CHA, as previously deduced with ANL<sup>16</sup>.

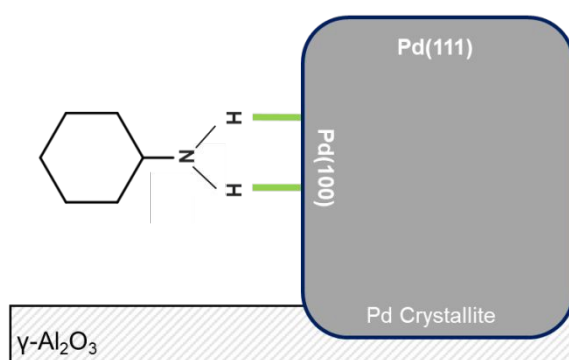


**Figure 5.** Visualisation of vertical CHA bonding to Pd(100).

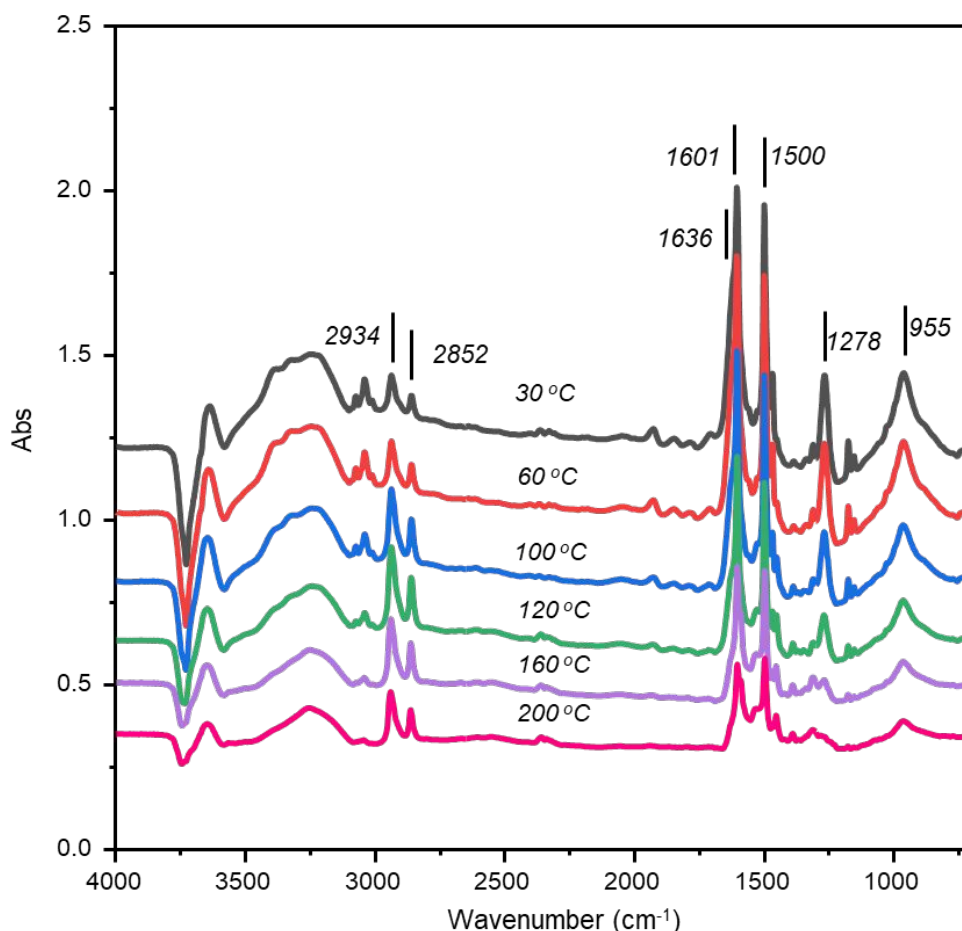


### 3.3 Temperature-Programmed IR: Aniline and H<sub>2</sub> Desorption from Pd/Al<sub>2</sub>O<sub>3</sub>

TP-IR spectra following co-adsorption of aniline and hydrogen (4.86<sub>(ANL)</sub> + 122<sub>(H<sub>2</sub>)</sub> mmol g(cat)<sup>-1</sup>) on Pd/Al<sub>2</sub>O<sub>3</sub> are shown in Figure 6. Aniline bands decreased progressively with temperature, yet no orientational change was observed; key in-plane ( $\nu(\text{Ph-NH}_2)$ ,  $\nu_{24}$  v(CC),  $\nu_4$  v(CC) at 1278, 1500, 1601 cm<sup>-1</sup>) and out-of-plane ( $\delta_{\text{oop}}(\text{NH}_2)$  at 1636 cm<sup>-1</sup>) modes remained distinct throughout desorption. A negative hydroxyl feature near 3730 cm<sup>-1</sup> persisted even after heating to 200 °C, indicating residual aniline bound to alumina hydroxyls.

Interestingly, CHA bands initially intensified during heating. Peak area trends (Figure 7) show an inverse relationship: ANL  $\nu(\text{Ph-NH}_2)$  decreases while CHA  $\nu_s(\text{CH}_2)$  increases between 30–120 °C, confirming hydrogenation of interfacial aniline at this temperature range to CHA. CHA formation ceases beyond 160 °C, marking the temperature range (120–160 °C) where aniline desorbs from Pd(100)/support sites.





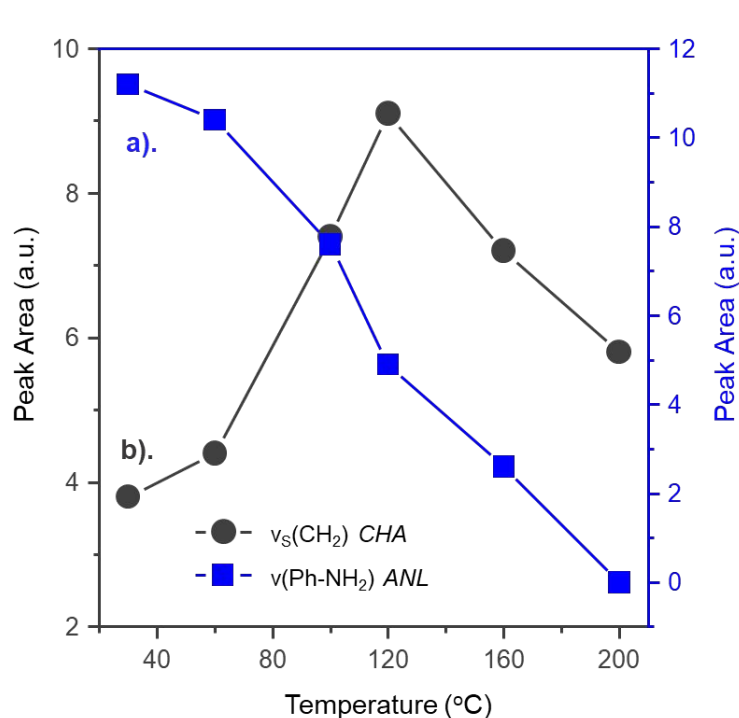
View Article Online  
DOI: 10.1039/D5FD00169B

**Figure 6.** TP-IR DRIFTS spectra (4000 – 700  $\text{cm}^{-1}$ ) of aniline and hydrogen adsorbed to  $\text{Pd}/\text{Al}_2\text{O}_3$  as a function of increasing temperature: 30 – 200  $^\circ\text{C}$ . The spectra have been offset to facilitate viewing.

Figure 6 shows some broadening at *ca.* 1640  $\text{cm}^{-1}$  was observed for temperatures  $\geq 160$   $^\circ\text{C}$ . This is assigned to the shifted in-plane  $\delta_{\text{ip}}(\text{NH}_2)$  mode of CHA that previously was associated with an element of CHA adsorption to the metal. The intensity of this feature compared to the  $\nu_{\text{AS}}(\text{CH}_2)$  and  $\nu_{\text{S}}(\text{CH}_2)$  modes (2936 and 2852  $\text{cm}^{-1}$ ) is far weaker than observed for low aniline and hydrogen exposures over the catalyst (Figure 1). Therefore, the presence of the shifted  $\delta_{\text{ip}}(\text{NH}_2)$  mode indicates some retention of CHA adsorption to the metal at this temperature, with the dominant CHA population residing on type IIa and type IIb hydroxyl groups of the alumina support.

After desorption at the maximum temperature, the medium intensity  $\nu(\text{Ph-NH}_2)$  mode of aniline was no longer distinct; however, the high intensity  $\nu_{24}(\text{CC})$  and  $\nu_4(\text{CC})$  modes remained (Table S1). Thus, a limited population of aniline remained adsorbed to the OH groups of the alumina support after desorption at 200  $^\circ\text{C}$ , such that the medium intensity  $\nu(\text{Ph-NH}_2)$  was not observed. A greater quantity of CHA remained.





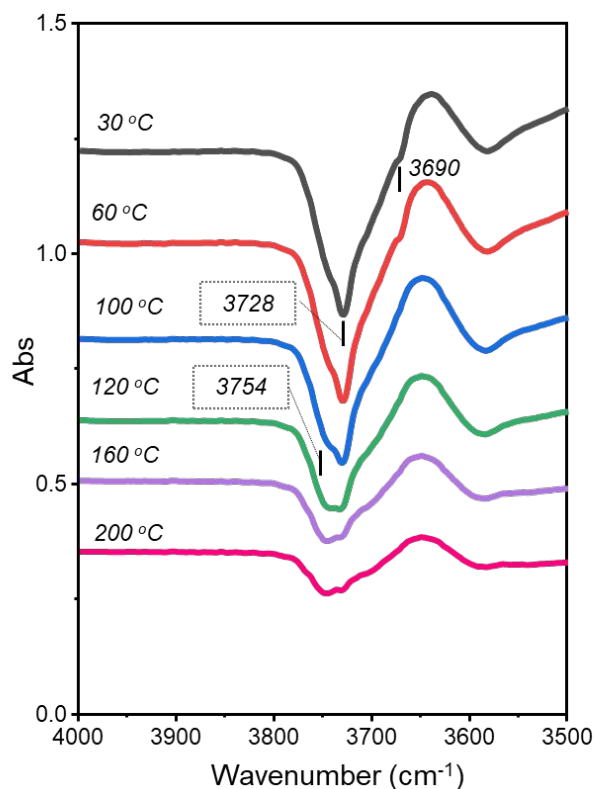
View Article Online  
DOI: 10.1039/D5FD00169B

**Figure 7.** Plot of peak area for bands corresponding to the a). aniline  $v(\text{Ph-NH}_2)$  and b). cyclohexylamine  $v_s(\text{CH}_2)$  modes as a function of increasing desorption temperature.

From consideration of the hydroxyl region of Figure 8, prior to temperature ramping (30 °C spectrum) two negative features were observed at 3728 and 3690  $\text{cm}^{-1}$  that correspond to aniline/CHA H-bonding to type IIb and type III hydroxyls, respectively. Upon increasing the desorption temperature to 100 °C, the hydroxyl region is resolved such that the band corresponding to aniline/CHA H-bonding with type IIa hydroxyls at 3754  $\text{cm}^{-1}$  was also distinct. Also, the feature aligned with H-bonding to type III hydroxyls was not observed; thus, aniline/CHA H-bonded to type III hydroxyls was desorbed in the temperature range of 60 – 100 °C.

Contrarily to sole aniline adsorption TP-IR measurements<sup>16</sup>, the profiles associated with spectra from aniline and hydrogen adsorption to Pd/Al<sub>2</sub>O<sub>3</sub> collected post-desorption at 160 and 200 °C clearly depict the type IIa OH site (3754  $\text{cm}^{-1}$ ) to be the dominant H-bonding adsorption site for this temperature range. This indicates stronger hydrogen-bonding of CHA with the hydroxyl support than aniline.





View Article Online  
DOI: 10.1039/D5FD00169B

**Figure 8.** DRIFTS spectra ( $4000 - 3500 \text{ cm}^{-1}$ ) depicting the hydroxyl group stretching region during increasing temperature ( $30 - 200 \text{ }^\circ\text{C}$ ) post aniline and hydrogen co-adsorption to  $\text{Pd}/\text{Al}_2\text{O}_3$ . The spectra have been offset to facilitate viewing.

The updated binding strength hierarchy for ANL and CHA on  $\text{Pd}/\text{Al}_2\text{O}_3$  is: Type III OH (ANL/CHA) < Pd(100)/support interface (ANL) < Pd(100) (CHA) < Type IIb OH (ANL/CHA) < Type IIa OH (ANL/CHA).

## 4. Discussion

Historically, aniline over-hydrogenation to CHA, DICHAN and CHAN has been the dominant route to lowered aniline selectivity during nitrobenzene hydrogenation<sup>2,6,8,9</sup>, with hydrogen loading identified as the dominant factor driving aniline hydrogenation over  $\text{Pd}/\text{Al}_2\text{O}_3$ <sup>16</sup>. Since this transformation represents the primary route to by-product formation, understanding its origin is essential for optimizing selectivity in nitrobenzene hydrogenation. Figure 9 schematically illustrates the adsorption complexity underpinning these outcomes. Insights from this paper and collective works of the authors<sup>8,15</sup> presents the following framework:

- (i) Nitrobenzene adsorbs on Pd(111) planes via monodentate binding in a vertical or slightly tilted orientation, limiting aromatic ring hydrogenation and suppressing nitrobenzene derived by-products.
- (ii) In the presence of hydrogen, nitrobenzene predominantly converts to aniline.



**(iii)** Aniline can re-adsorb at Pd(100)/support interfacial sites in a parallel orientation, interacting through its nitrogen lone pair with Pd and forming H-bonds with adjacent alumina hydroxyls.

View Article Online

DOI: 10.1039/D5FD00169B

**(iv)** Aniline predominantly adsorbs on type IIa, IIb, and III hydroxyl groups of the alumina support. This preference for the inactive support restricts further hydrogenation, explaining the inherent selectivity of Pd/Al<sub>2</sub>O<sub>3</sub> catalysts for aniline synthesis.

**(v)** Aniline adsorbed in a parallel orientation at Pd(100)/support interfaces undergoes hydrogenation to CHA, enabled by the planar alignment of the aromatic ring with the active Pd surface.

**(vi)** CHA can re-adsorb vertically on Pd(100) via bidentate binding.

**(vii)** CHA also resides on type IIa, IIb, and III hydroxyl sites of the alumina support, where strong H-bonding prevents further transformation to N-cyclohexylcyclohexylaniline (CHAN).

Collectively, these observations reveal a sequence of adsorption and transformation steps that govern selectivity: nitrobenzene activation on Pd(111), aniline formation and interfacial hydrogenation on Pd(100), and eventual stabilization of CHA on alumina hydroxyls. This interplay between metal and support sites explains why Pd/Al<sub>2</sub>O<sub>3</sub> catalysts favour aniline synthesis and limit deeper hydrogenation. The mechanistic picture presented here provides a foundation for rational catalyst design and indicates the suitability of Pd/Al<sub>2</sub>O<sub>3</sub> as a candidate aniline synthesis catalyst.



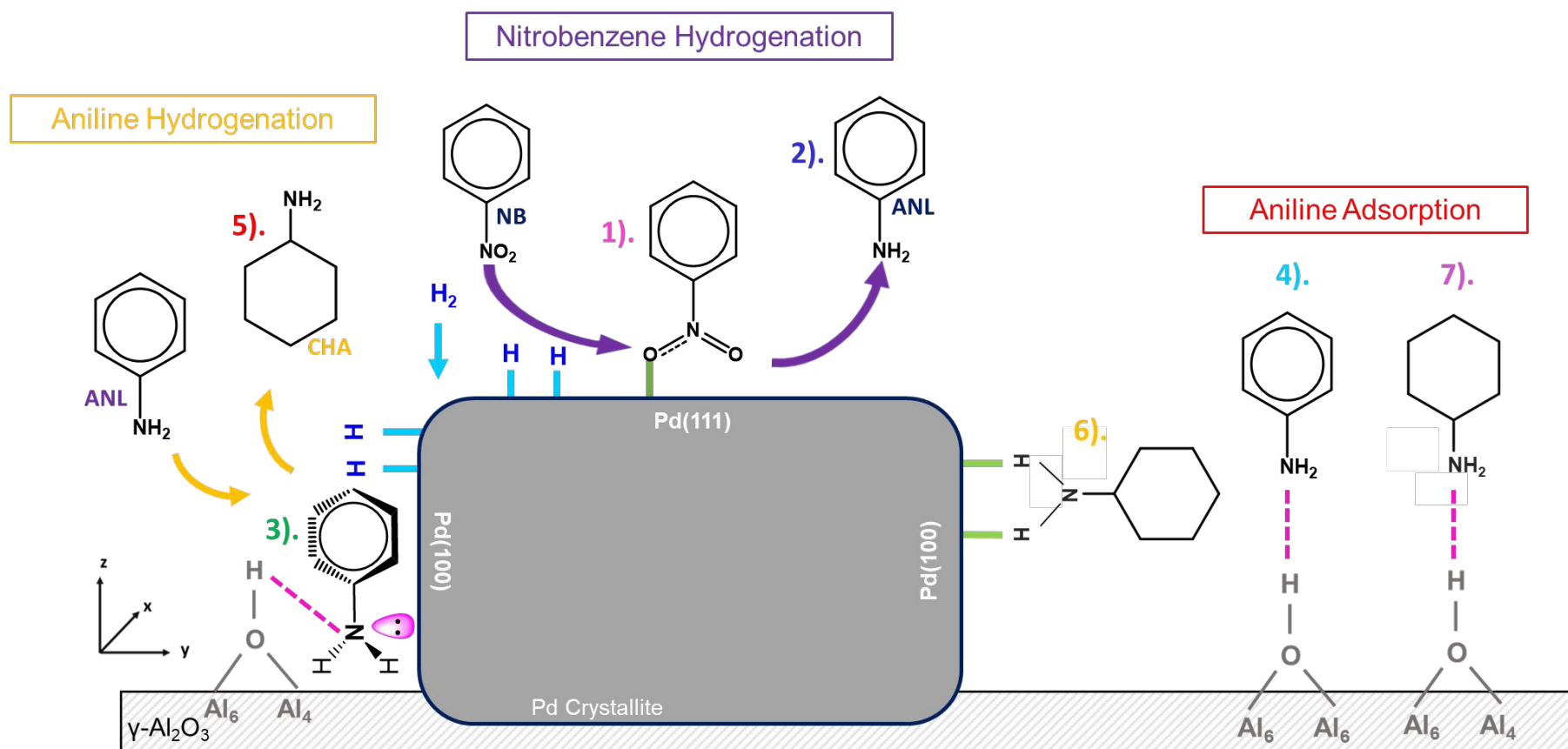


**Figure 9.** Diagram visualising nitrobenzene (NB) adsorption to Pd(111) in a vertical orientation via one Pd-O bond, with subsequent hydrogenation to aniline (ANL), parallel aniline adsorption with respect to the metal at the support/Pd(100) interface, , hydrogenation of parallel adsorbed aniline to cyclohexylamine, vertical bidentate CHA adsorption on Pd(100) and adsorption of aniline and CHA to the support with no specific geometry identified. The solid grey box represents a non-specific Pd crystallite; the hashed box represents the support. Larger arrows for vertical NB hydrogenation to ANL depicts this as the major transformation.

## 5. Conclusions

View Article Online  
DOI: 10.1039/D5FD00169B

Infrared spectroscopy combined with application of the MSSR, enabled the derivation of a detailed structure–activity relationship governing selective aniline synthesis over Pd/Al<sub>2</sub>O<sub>3</sub> catalysts. This approach demonstrates how catalytic selectivity can be rationalized from fundamental IR principles. The key conclusions are as follows:

- **Hydroxyl site interactions:** Strong negative OH features at 3754, 3728, and 3690 cm<sup>-1</sup> confirm adsorption of aniline and CHA on type IIa, IIb, and III hydroxyl groups of the γ-Al<sub>2</sub>O<sub>3</sub> support.
- **Low-coverage adsorption geometry:** At ≤0.54(ANL)+13.5(H<sub>2</sub>) mmol g(cat)<sup>-1</sup>, spectra show only out-of-plane aniline modes and negative OH features, consistent with parallel adsorption at Pd/support interfacial sites.
- **CHA formation:** Bands at 2934 and 2852 cm<sup>-1</sup>, assigned to ν<sub>AS</sub>(CH<sub>2</sub>) and ν<sub>S</sub>(CH<sub>2</sub>), appear at exposures ≥1.08(ANL)+27.0(H<sub>2</sub>) mmol g(cat)<sup>-1</sup>, indicating hydrogenation of adsorbed aniline to CHA.
- **Combined NH<sub>2</sub> deformation features:** Enlargement of the broad band near 1650 cm<sup>-1</sup> under the hydrogen co-feed reflects overlapping δ<sub>oop</sub>(NH<sub>2</sub>) (aniline) and δ<sub>ip</sub>(NH<sub>2</sub>) (CHA) modes, indicative of NH<sub>2</sub>-mediated binding to Pd surfaces.
- **CHA orientation:** Enhanced δ<sub>ip</sub>(NH<sub>2</sub>) intensity relative to out-of-plane CH<sub>2</sub> stretches at low coverage indicates vertical CHA adsorption on Pd(100).
- **High-coverage behaviour:** At exposures of ≥1.13(ANL)+28.4(H<sub>2</sub>) mmol g(cat)<sup>-1</sup>, all aniline modes appear alongside intensified OH features, confirming adsorption shifts to alumina hydroxyls. CHA modes dominate, indicating CHA stabilization on the support.
- **Site differentiation:** Peak-area trends and TP-IR confirm CHA occupies additional sites beyond those of aniline, including Pd(100) planes, where CHA adsorbs vertically.
- **Binding hierarchy:** TP-IR establishes the order of adsorption strength: Type III OH (ANL/CHA) < Pd(100)/support interface (ANL) < Pd(100) (CHA) < Type IIb OH (ANL/CHA) < Type IIa OH (ANL/CHA).

Overall, these findings reveal that hydrogen loading drives CHA formation via interfacial aniline hydrogenation, while strong aniline adsorption on alumina hydroxyls limits deeper hydrogenation. This mechanistic understanding provides a basis for rational catalyst design.



## Acknowledgements

The EPSRC are thanked for the provision of a Ph.D. studentship (ALMcC, EP/R513222/1 & EP/N509668/1). View Article Online  
DOI: 10.1039/C5FD00169B

## Author's Contribution

**Annelouise McCullagh:** Methodology, Formal analysis, Investigation, Data Curation, Writing - Original Draft, Writing - Review & Editing; **David Lennon:** Conceptualization, Methodology, Resources, Writing - Review & Editing, Supervision, Project administration, Funding acquisition.

## Data Management Statement

Datasets for the article will be available at the University of Glasgow Library from March 2026.

## Conflicts of Interest.

There are no conflicts of Interest.



## References

View Article Online  
DOI: 10.1039/D5FD00169B

- (1) Kahl, T.; Schröder, K. W.; Lawrence, F.; Marshall, W.; Höke, H.; Jäckh, R. Aniline. In *Ullmann's Encyclopedia of Industrial Chemistry*; Wiley: Weinheim, 2012; pp 45–478.
- (2) Couto, C. S.; Madeira, L. M.; Nunes, C. P.; Araújo, P. Hydrogenation of Nitrobenzene over a Pd/Al<sub>2</sub>O<sub>3</sub> Catalyst – Mechanism and Effect of the Main Operating Conditions. *Chem. Eng. Technol.* **2015**, *38* (9), 1625–1636. <https://doi.org/10.1002/ceat.201400468>.
- (3) Gelder, E. A.; Jackson, S. D.; Lok, C. M. The Hydrogenation of Nitrobenzene to Aniline: A New Mechanism. *Chem. Commun.* **2005**, No. 4, 522–524. <https://doi.org/10.1039/B411603H>.
- (4) Kataoka, S.; Takeuchi, Y.; Harada, A.; Takagi, T.; Takenaka, Y.; Fukaya, N.; Yasuda, H.; Ohmori, T.; Endo, A. Microreactor Containing Platinum Nanoparticles for Nitrobenzene Hydrogenation. *Appl. Catal. Gen.* **2012**, *427–428*, 119–124. <https://doi.org/10.1016/j.apcata.2012.03.041>.
- (5) Jiang, H.; Yuan, G.; Cui, Z.; Zhao, Z.; Dong, Z.; Zhang, J.; Cong, Y.; Li, X. Effects of Support Types and Their Porosity Characteristics on the Catalytic Performance of Ni-Based Catalysts in Nitrobenzene Hydrogenation to Aniline. *Ind. Eng. Chem. Res.* **2023**, *62* (34), 13355–13367. <https://doi.org/10.1021/acs.iecr.3c01327>.
- (6) Morisse, C. G. A.; McCullagh, A. M.; Campbell, J. W.; Mitchell, C.; Carr, R. H.; Lennon, D. Mechanistic Insight Into the Application of Alumina-Supported Pd Catalysts for the Hydrogenation of Nitrobenzene to Aniline. *Ind. Eng. Chem. Res.* **2022**, *61* (30), 10712–10722. <https://doi.org/10.1021/acs.iecr.2c01134>.
- (7) Brereton, G. Polyurethanes. In *Ullmann's Encyclopedia of Industrial Chemistry*; Wiley: Weinheim, 2019; pp 1–76.
- (8) Campbell, J. W.; McCullagh, A. M.; McGrath, L.; How, C.; MacLaren, D. A.; Loenders, M.; Meyer, N.; Carr, R. H.; Lennon, D. The Application of Alumina Supported Pd Catalysts for High Selectivity Aniline Synthesis Catalysis at Elevated Temperatures: Site-Selective Chemistry. *Appl. Catal. Gen.* **2024**, *670*, 119541. <https://doi.org/10.1016/j.apcata.2023.119541>.
- (9) Morisse, C. G. A.; McCullagh, A. M.; Campbell, J. W.; How, C.; MacLaren, D. A.; Carr, R. H.; Mitchell, C. J.; Lennon, D. Toward High Selectivity Aniline Synthesis Catalysis at Elevated



Temperatures. *Ind. Eng. Chem. Res.* **2021**, *60* (49), 17917–17927.  
<https://doi.org/10.1021/acs.iecr.1c03695>.

View Article Online  
DOI: 10.1039/D5FD00169B

- (10) Rockey, T. J.; Yang, M.; Dai, H.-L. Aniline on Ag(1 1 1): Adsorption Configuration, Adsorbate–Substrate Bond, and Inter-Adsorbate Interactions. *Surf. Sci.* **2005**, *589* (1), 42–51. <https://doi.org/10.1016/j.susc.2005.05.048>.
- (11) Huang, S. X.; Fischer, D. A.; Gland, J. L. Correlation between the Surface Configurations and Hydrogenolysis: Aniline on the Pt(111) Surface. *J. Vac. Sci. Technol. A* **1994**, *12* (4), 2164–2169. <https://doi.org/10.1116/1.579107>.
- (12) Alsunaidi, Z. H. A.; Cundari, T. R.; Wilson, A. K. Toward a More Rational Design of the Direct Synthesis of Aniline: A Density Functional Theory Study. *ACS Omega* **2017**, *2* (7), 3214–3227. <https://doi.org/10.1021/acsomega.7b00356>.
- (13) *Computational Investigation of Precursor Blocking during Area-Selective Atomic Layer Deposition Using Aniline as a Small-Molecule Inhibitor | Langmuir.* <https://pubs.acs.org/doi/10.1021/acs.langmuir.2c03214> (accessed 2025-11-26).
- (14) Henríquez-Román, J. H.; Padilla-Campos, L.; Páez, M. A.; Zagal, J. H.; Rubio, M. A.; Rangel, C. M.; Costamagna, J.; Cárdenas-Jirón, G. The Influence of Aniline and Its Derivatives on the Corrosion Behaviour of Copper in Acid Solution: A Theoretical Approach. *J. Mol. Struct. THEOCHEM* **2005**, *757* (1), 1–7. <https://doi.org/10.1016/j.theochem.2005.05.018>.
- (15) McCullagh, A. M.; Gibson, E. K.; Parker, S. F.; Refson, K.; Lennon, D. The Adsorption of Nitrobenzene over an Alumina-Supported Palladium Catalyst: An Infrared Spectroscopic Study. *Phys. Chem. Chem. Phys.* **2023**, *25* (38), 25993–26005. <https://doi.org/10.1039/D3CP03028H>.
- (16) McCullagh, A. M.; Parker, S. F.; Lennon, D. The Adsorption of Aniline over Alumina-Supported Palladium: An Infrared Spectroscopic and Computational Study. *Philosophical Transactions of the Royal Society A* **2026**. <https://doi.org/DOI:%252010.1098/rsta.2024.0556>.
- (17) McCullagh, A. M.; Lennon, D. The Hydrogenation of Aniline over an Alumina-Supported Pd Catalyst. *Submitted for publication, December 2025*.
- (18) Chen, J.-Y. T.; Gould, J. H. Infrared Studies of Cyclohexylamine. *J. Assoc. Off. Anal. Chem.* **1972**, *55* (5), 1006–1014. <https://doi.org/10.1093/jaoac/55.5.1006>.



- (19) Darkhalil, I. D.; Klaassen, J. J.; Deodhar, B. S.; Gounev, T. K.; Durig, J. R. Conformational Stability, Infrared and Raman Spectra, Vibrational Assignments, and Theoretical Calculations of Cyclohexylamine. *J. Mol. Struct.* **2015**, *1088*, 169–178. <https://doi.org/10.1016/j.molstruc.2015.02.007>. View Article Online  
DOI: 10.1039/C5FD00169B
- (20) Knozinger, H.; Ratnasamy, P. Catalytic Aluminas: Surface Models and Characterisation of Surface Sites. *Sci and Eng* **1978**, *17*, 31–70. <https://doi.org/doi.org/10.1080/03602457808080878>.
- (21) Greenler, R. G.; Snider, D. R.; Witt, D.; Sorbello, R. S. The Metal-Surface Selection Rule for Infrared Spectra of Molecules Adsorbed on Small Metal Particles. *Surf. Sci.* **1982**, *118* (3), 415–428. [https://doi.org/10.1016/0039-6028\(82\)90197-2](https://doi.org/10.1016/0039-6028(82)90197-2).



### Data Management Statement

Datasets for the article will be available at the University of Glasgow Library from February 2026

[View Article Online](#)  
DOI: 10.1039/D5FD00169B

D. Lennon (15<sup>th</sup> December 2025).

